Available online at www.sciencedirect.com
ScienceDirect
Journal of Power Sources 165 (2007) 728–732
JOURNAL OF POWER SOURCES
www.elsevier.com/locate/jpowsour

Short communication

Synthesis of nano-crystalline $(Ba_{0.5}Sr_{0.5})Co_{0.8}Fe_{0.2}O_{3-\delta}$ cathode material by a novel sol–gel thermolysis process for IT-SOFCs

A. Subramania [a,*], T. Saradha [a], S. Muzhumathi [b]

[a] *Advanced Materials Research Laboratory, Department of Industrial Chemistry, Alagappa University, Karaikudi 630003, India*
[b] *Fuel Cell Division, Central Electrochemical Research Institute, Karaikudi 630006, India*

Received 18 October 2006; received in revised form 21 December 2006; accepted 21 December 2006
Available online 12 January 2007

Abstract

Nano-crystalline $(Ba_{0.5}Sr_{0.5})Co_{0.8}Fe_{0.2}O_{3-\delta}$ powder has been successfully synthesized by a novel sol–gel thermolysis method using a unique combination of PVA and urea. The decomposition and crystallization behaviour of the gel precursor was studied by TG/DTA analysis. The gel precursor was calcined at different temperatures and the phase evoluation was studied by X-ray diffraction (XRD) analysis. From the result of X-ray diffraction patterns, it is found that a cubic perovskite $(Ba_{0.5}Sr_{0.5})Co_{0.8}Fe_{0.2}O_{3-\delta}$ was formed by calcining the precursor at 450 °C for 5 h, but the well-crystalline cubic perovskite $(Ba_{0.5}Sr_{0.5})Co_{0.8}Fe_{0.2}O_{3-\delta}$ was obtained by calcining the precursor at 650 °C for 5 h. Morphological analysis of the powder calcined at various temperatures was done by scanning electron microscope (SEM). Thermogravimetric (TG) results showed the lattice oxygen loss of the product was about ∼2% in its original weight in the temperature range 40–900 °C. Finally, thermal expansion and electrical conductivity of the synthesized material were measured by dilatometer and four-probe dc method, respectively.

Keywords: $(Ba_{0.5}Sr_{0.5})Co_{0.8}Fe_{0.2}O_{3-\delta}$; Sol–gel thermolysis process; Nano-crystalline powder; IT-SOFC cathode material

1. Introduction

Solid oxide fuel cells (SOFC) are considered as one of the most promising energy conversion devices that exhibit advantages such as high efficiency, system compactness and low environmental pollution [1–3]. The traditional SOFC must operated at high temperature (around 1000 °C), which causes many problems include a degradation of performance due to the formation of second phase, sintering of the electrode and interfacial diffusion between electrode and electrolyte. Therefore, a common trend is to develop reduced temperature SOFC systems which can be operated at lower temperature, typically below 800 °C. So intermediate-temperature solid oxide fuel cells (IT-SOFC) have attracted much attention in recent years [4–6]. However, a major issue with the reduced operating temperature is the decrease in the catalytic activity of the cathode for oxygen reduction [7]. The state-of-the-art cathode material for high temperature (∼1000 °C) operation is the $La_{1-x}Sr_xMnO_3$ perovskite oxide. However, its poor oxide ion conductivity prevents its use for intermediate temperature SOFC [8,9]. Development of alternative cathode materials with adequate mixed ionic-electronic conductivity (MIEC) is needed to make the intermediate temperature SOFC technology successful. In this regard, very recently, Shao et al. reported a new material $(Ba_{0.5}Sr_{0.5})Co_{0.8}Fe_{0.2}O_{3-\delta}$ (BSCF), which showed excellent performance as the cathode material in conjunction with ceria-based electrolytes at reduced temperatures compared to conventional cathode materials [10]. But the synthesis of $(Ba_{0.5}Sr_{0.5})Co_{0.8}Fe_{0.2}O_{3-\delta}$ is generally carried out by the traditional solid-state reaction method [11], and wet chemical methods, such as modified citrate [11] and citrate-EDTA complexing method [10–13]. Although these methods are time consuming and require higher calcining temperature (about 950 °C), long time to prepare the precursor, which raises the difficulties in preparing homogeneous material with good reproducibility. To overcome these difficulties a novel sol–gel thermolysis method is introduced for the synthesis of high pure BSCF nano-powder for the large scale. This sol–gel thermolysis process is a unique combination of a thermolysis process and a chemical gelation process. The organic polymer(s) not only act as an excellent fuel, but also controls the particle size

* Corresponding author. Tel.: +91 4565 228836; fax: +91 4565 225202.
E-mail address: a_subramania@yahoo.co.in (A. Subramania).

0378-7753/$ – see front matter © 2007 Elsevier B.V. All rights reserved.
doi:10.1016/j.jpowsour.2006.12.067

during the formation of gelation process and also prevents the aggregation of particles during the thermolysis of dry gel due to its long chain structure. In this context, we have reported very recently, the synthesis of nano-crystalline $LiSr_xMn_{2-x}O_4$ powders by a novel sol–gel thermolysis process using PVA and urea combination for Li-ion batteries [14].

Herein, we intended to use this method for synthesis of nano-crystalline $(Ba_{0.5}Sr_{0.5})Co_{0.8}Fe_{0.2}O_{3-\delta}$ powder using a unique combination of PVA and urea. The thermal decomposition behaviour of gel precursor was examined by TG/DTA analysis. Formation of crystalline phase of the powder on calcination at various temperatures was confirmed by X-ray diffraction analysis. The morphology of the powder was characterized by scanning electron microscopy (SEM). Finally, the weight loss with temperature, thermal expansion behaviour and electrical conductivity of $(Ba_{0.5}Sr_{0.5})Co_{0.8}Fe_{0.2}O_{3-\delta}$ were also studied.

2. Experimental

2.1. Synthesis of $(Ba_{0.5}Sr_{0.5})Co_{0.8}Fe_{0.2}O_{3-\delta}$ powder

The nano-crystalline $(Ba_{0.5}Sr_{0.5})Co_{0.8}Fe_{0.2}O_{3-\delta}$ powder was synthesized by a novel sol–gel thermolysis process using urea as the fuel for combustion process and PVA as the dispersing agent as well as secondary fuel. The experimental procedure for the synthesis of $(Ba_{0.5}Sr_{0.5})Co_{0.8}Fe_{0.2}O_{3-\delta}$ is depicted as the flow chart is shown in Fig. 1. In this method, stoichiometric amount of nitrates of Ba, Sr, Co and Fe were dissolved in triple distilled water. To this, aqueous solution

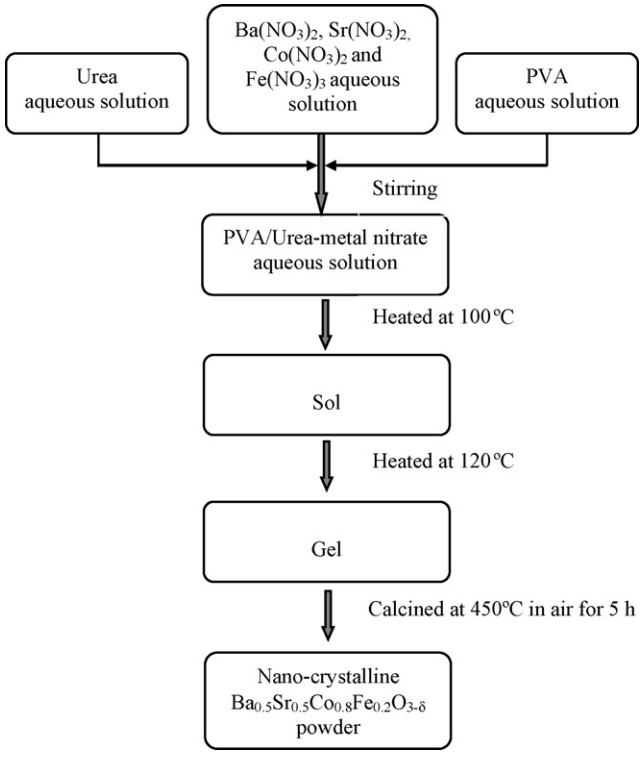

Fig. 1. Flowchart for the preparation of nano-crystalline $(Ba_{0.5}Sr_{0.5})Co_{0.8}Fe_{0.2}O_{3-\delta}$ powder by sol–gel thermolysis process.

of PVA and urea were added with constant stirring until a homogeneous solution was achieved. The stoichiometry amount of the redox mixture used for the combustion reaction was calculated based on the total oxidizing (O) and reducing (F) valencies of the components which serve as the numerical coefficient for the stoichiometric balance to equivalent ratio (ϕ_e) was maintained at unity (O/F), so that the heat released by the combustion is maximum [15]. According to the concepts used in propellent chemistry, the oxidizing valency of $Ba(NO_3)_2$ is -10, $Sr(NO_3)_2$ is -10, $Co(NO_3)_2$ is -10, $Fe(NO_3)_3$ is -15 and reducing valencies of urea is +6 [16]. The amount of urea required for combustion is calculated using the general empirical formula for the system $(Ba_{0.5}Sr_{0.5})Co_{0.8}Fe_{0.2}O_{3-\delta}$ is $(0.5\times(-10))+(0.5\times(-10))+(0.8\times(-10))+(0.2\times(-15))+6n=0$; $n=3.5$ M. Hence, the required amount of urea is 3.5 M and also the amount of PVA is just equal to that the amount of urea taken. The above-obtained solution was then heated to 100 °C to obtain a viscous solution (sol). This viscous solution was again heated to 120 °C for 3 h to obtain the precursor sample (gel). Finally, the obtained precursor sample was calcined at various temperatures, viz. 450, 550 and 650 °C for 5 h in air to obtain a single-phase nano-crystalline $(Ba_{0.5}Sr_{0.5})Co_{0.8}Fe_{0.2}O_{3-\delta}$ powder. This powder was then pressed into a green disk at about 200 MPa followed by sintering at 850 °C in air for 5 h to get dense sample.

2.2. Characterizations

The thermal decomposition behaviour of the precursor sample was studied by TG/DTA thermal analyzer (Model: Perkin-Elmer-Pyris Diamond) at the temperature range of 30–700 °C with a heating rate of 5 °C min^{-1} under an ordinary atmosphere. X-ray diffraction analysis (Model: Philips X'Pert MPD®) was carried out on the product obtained at various temperatures for phase purity and structural confirmation. The diffraction patterns were obtained at 25 °C in the range $20^\circ \le 2\theta \le 80^\circ$. The step size and scan rate were set at 0.1 and 2° min^{-1}, respectively. Microstructural analysis was carried by JEOL-scanning electron microscopy (Model: JSM-840A).

The change in weight loss of $(Ba_{0.5}Sr_{0.5})Co_{0.8}Fe_{0.2}O_{3-\delta}$ sample was measured by thermogravimetric (TG) analysis using Perkin-Elmer TG/DTA thermal analyzer (Model: Pyris Diamond) at the temperature range of 40–900 °C with a heating rate of 2 °C min^{-1} under an ordinary atmosphere.

Thermal expansion coefficient (TEC) was measured by a dilatometer (Netzsch DIL 402/3/G) in the temperature range of 40–900 °C with a heating rate of 2 °C min^{-1} in air. The electrical conductivity of the sample was measured by Four-probe dc method using (Keithley 2400) digital source meter with a programmed temperature controller at 40–900 °C in air.

3. Results and discussion

3.1. TG/DTA analysis

Fig. 2 shows the TG/DTA curves for $(Ba_{0.5}Sr_{0.5})Co_{0.8}Fe_{0.2}O_{3-\delta}$ precursor sample. The weight loss in the tempera-

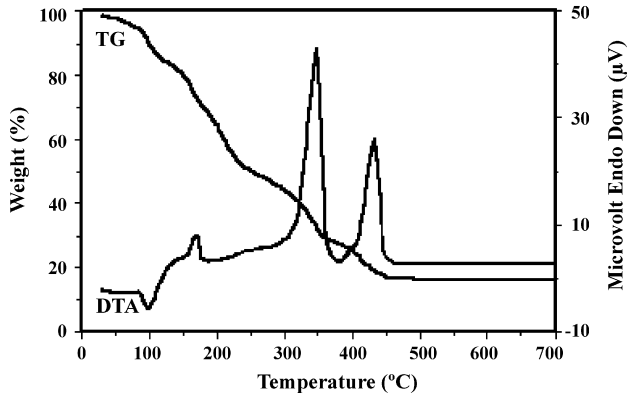

Fig. 2. TG/DTA curves $(Ba_{0.5}Sr_{0.5})Co_{0.8}Fe_{0.2}O_{3-\delta}$ gel precursor at a heating rate of 5 °C min^{-1}.

ture range 30–130 °C corresponds to the removal of superficial and structural water in the gel precursor, which is accompanied by small endothermic peak at 100 °C in the DTA curve. The weight loss in the temperature range 130–360 °C corresponds to the combustion of inorganic and organic constituents of the precursor, such as nitrates, urea and PVA, which occurs with the exothermic peaks at 173 and 349 °C in the DTA curve. The small weight loss at temperature above 360 °C is associated with the crystallization of cubic perovskite $(Ba_{0.5}Sr_{0.5})Co_{0.8}Fe_{0.2}O_{3-\delta}$, accompanied by the exothermic peak at 430 °C in the DTA curve. Almost no weight loss was observed above 450 °C, implying only the presence of $(Ba_{0.5}Sr_{0.5})Co_{0.8}Fe_{0.2}O_{3-\delta}$. It was further confirmed by XRD measurements.

3.2. X-ray diffraction studies

The X-ray diffraction (XRD) patterns for the precursor sample calcined at various temperatures for 5 h in air are shown in Fig. 3. For the material calcined at 450 °C for 5 h, a single-phase $(Ba_{0.5}Sr_{0.5})Co_{0.8}Fe_{0.2}O_{3-\delta}$ is formed, without any other noticeable impurity phase. But the diffraction peaks are much broader, which can be eliminated by further calcination at above 550 °C and at the calcination temperature of 650 °C, diffraction peaks become sharper with an increase in intensity. This suggests a gradual growth in the average particle size with an increase in crystallinity of $(Ba_{0.5}Sr_{0.5})Co_{0.8}Fe_{0.2}O_{3-\delta}$ powder. The average crystallite size at various temperatures was calculated using Scherrer's formula [17] and is presented in Table 1. The precursor is crystallized into phase-pure $(Ba_{0.5}Sr_{0.5})Co_{0.8}Fe_{0.2}O_{3-\delta}$ cubic perovskite powder with no minor phase formation throughout the calcination temperature range. All the XRD patterns were well indexed as a cubic perovskite structure with a space group of *Pm*3*m*(2 2 1). These results strongly suggests that sol–gel thermolysis process requires much lower calcination temperature with shorter time duration than other reported methods [10–13], where the calcination temperature is usually 800–1000 °C for more than 5 h. These results clearly indicated that the use of PVA/urea greatly suppressed the formation of precipitates leading to heterogeneity, since the gel precursor may provide good homogeneous mixing of the cations with no segregation during calcinations.

Table 1
Average crstallite size of $(Ba_{0.5}Sr_{0.5})Co_{0.8}Fe_{0.2}O_{3-\delta}$ powder synthesized by sol–gel thermolysis process

Calcination temperature (°C)	Average crystallite size (nm)
450	34
550	45
650	57

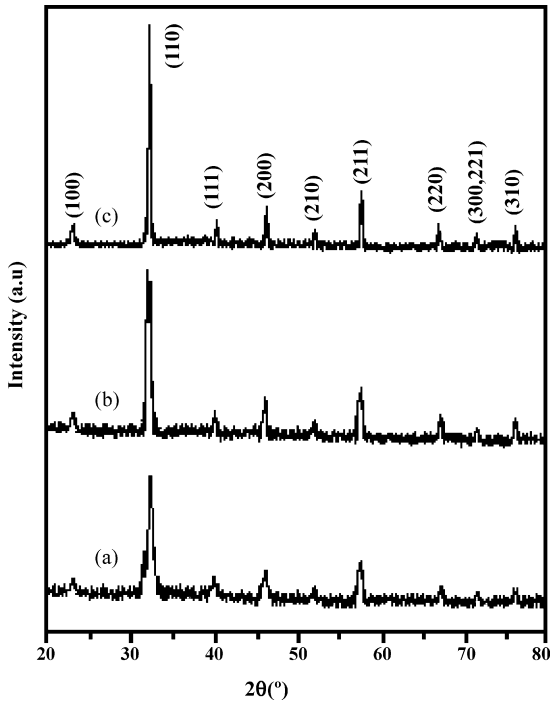

Fig. 3. XRD patterns for the gel precursor sample calcined at various temperatures: (a) 450 °C, (b) 550 °C and (c) 650 °C.

3.3. SEM analysis

Scanning electron micrographs of $(Ba_{0.5}Sr_{0.5})Co_{0.8}Fe_{0.2}O_{3-\delta}$ powder calcined at various temperatures for 5 h are shown in Fig. 4(a–c). The presence of highly porous spherical particles with a nano-metric grain size is detected in powder calcined at 450 °C (Fig. 4a). As the calcination temperature increases, growth kinetics are favoured and thus the spherical particles became larger, but the structure remained porous, which resembled the typical cathode structure for SOFC.

3.4. Thermogravimetric analysis

Fig. 5 shows the TGA plots of $(Ba_{0.5}Sr_{0.5})Co_{0.8}Fe_{0.2}O_{3-\delta}$ powder as a function of temperature upon heating. The observed weight loss during heating is due to the loss of oxygen from the lattice, which results in the formation of oxygen vacancies and the valence change of the metal ions [18], according to the defect

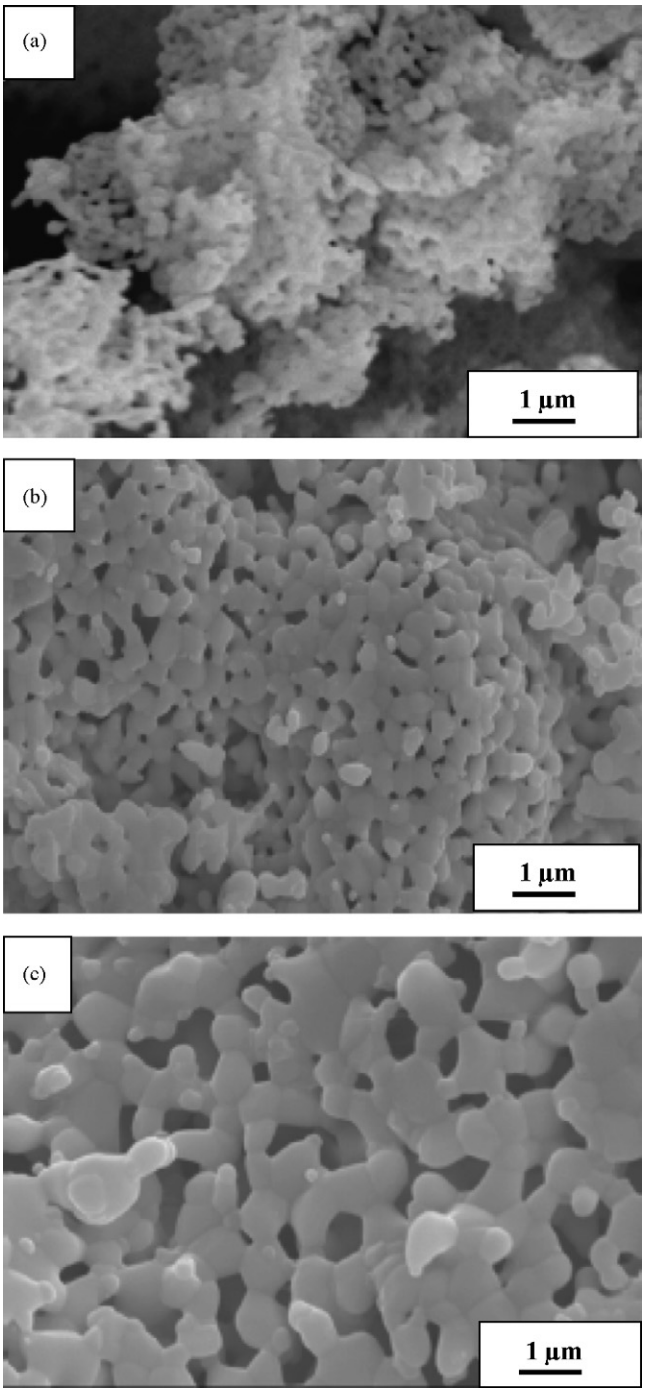

Fig. 4. Scanning electron micrographs of $(Ba_{0.5}Sr_{0.5})Co0_{.8}Fe_{0.2}O_{3-\delta}$ powder calcined at: (a) 450 °C, (b) 550 °C and (c) 650 °C.

reaction written in the Kroger–Vink notation

$$2M_M^{\bullet} + O_O^X \overset{\Delta}{\rightleftarrows} 2M_M^X + V_O^{\bullet\bullet} + \tfrac{1}{2}O_2 \uparrow \quad (1)$$

Where M represents Fe or Co. The weight loss in the TGA curve in the temperature range 210–475 °C is high, indicating that the loss mechanism of lattice oxygen in this region becomes more active. It is closely associated with the reduction from higher valence state Co^{4+} and Fe^{4+} to lower valence state Co^{3+} and Fe^{3+}, accompanied by the loss of lattice oxygen, which can also

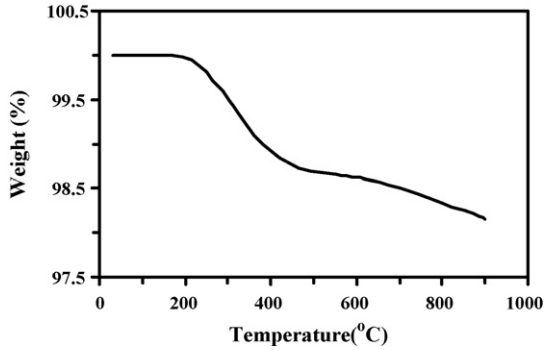

Fig. 5. TGA plot of $(Ba_{0.5}Sr_{0.5})Co_{0.8}Fe_{0.2}O_{3-\delta}$ recorded in air with a heating rate of 2 °C min^{-1}.

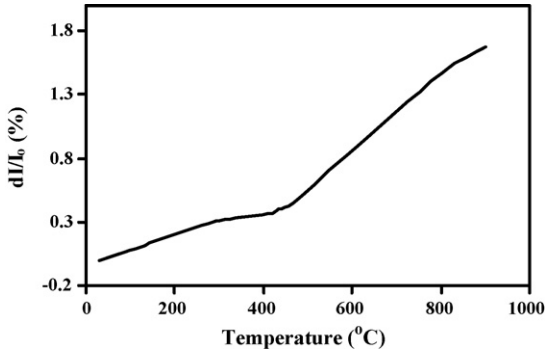

Fig. 6. Thermal expansion behaviour of $(Ba_{0.5}Sr_{0.5})Co_{0.8}Fe_{0.2}O_{3-\delta}$ at 40–900 °C in air.

be expressed as

$$2Co_{Co}^{\bullet} + O_O^X \rightleftarrows 2Co_{Co}^X + V_O^{\bullet\bullet} + \tfrac{1}{2}O_2 \uparrow \quad (2)$$

$$2Fe_{Fe}^{\bullet} + O_O^X \rightleftarrows 2Fe_{Fe}^X + V_O^{\bullet\bullet} + \tfrac{1}{2}O_2 \uparrow \quad (3)$$

Such thermal reductions occur simultaneously with the creation of oxygen vacancies in order to maintain the electrical neutrality.

3.5. Thermal expansion

Thermal expansion behaviour of $(Ba_{0.5}Sr_{0.5})Co_{0.8}Fe_{0.2}O_{3-\delta}$ at 40–900 °C in air is shown in Fig. 6. The thermal expansion curve is almost linear at 40–300 °C, and there is a significant inflection occurred in between 350 and 550 °C. The appearance of this inflection points occurred at such moderate temperature, can mainly be attributed to the loss of lattice oxygen and the formation of oxygen vacancies. Then, it is expected reduction of cations in the B-site, given in Eqs. (2) and (3), can cause a decrease in the B–O bond according to Pauling's second rule. Hence, the size of BO_6 octahedra increases, which enhance the lattice expansion [19].

3.6. Electrical conductivity

The logarithm of electrical conductivity ($\log\sigma$) of the system, $(Ba_{0.5}Sr_{0.5})Co_{0.8}Fe_{0.2}O_{3-\delta}$ is measured in the temperature range 40–900 °C in air is drawn as a function of reciprocal temperature is shown in Fig. 7. The perovskite

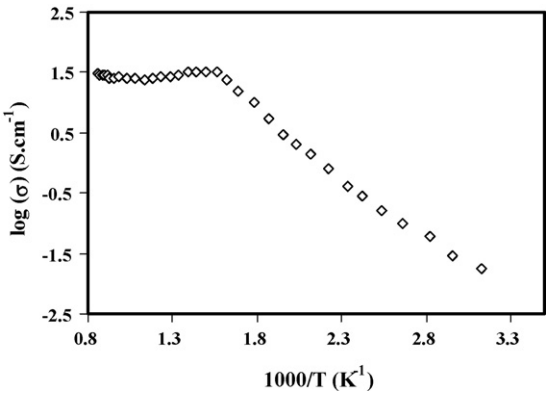

Fig. 7. Log σ vs. reciprocal temperature (1000/T) of $(Ba_{0.5}Sr_{0.5})Co_{0.8}Fe_{0.2}O_{3-\delta}$ in air.

$(Ba_{0.5}Sr_{0.5})Co_{0.8}Fe_{0.2}O_{3-\delta}$ is a mixed conductor; the total conductivity involves both electronic and ionic conductivity terms, due to the presence of holes and oxygen vacancies. The ionic conductivity is about two orders of magnitude lower than electronic conductivity, so it is reasonable to assume that the measured values mainly refer to the latter one [20]. As proved by thermopower measurement, the conductivity mechanism can be attributed to the hopping of p-type small polarons, which are associated with the behaviour of triple and tetravalent state of cobalt and iron cations. The electron transits between the triple and the tetravalent of Co and Fe causes the electronic conductivity. It can be seen that the electrical conductivity of $(Ba_{0.5}Sr_{0.5})Co_{0.8}Fe_{0.2}O_{3-\delta}$ is increased gradually with temperature and has the maximum electrical conductivity at about 350–500 °C. This is due to the behaviour of lattice oxygen that becomes active at this temperature range and this has good agreement with the TG and TEC results. The activation energy calculated from the linear part is 14.01 kJ mol^{-1} and it shows the maximum conductivity of 32 S cm^{-1} at 500 °C.

4. Conclusions

The phase-pure nano-crystalline $(Ba_{0.5}Sr_{0.5})Co_{0.8}Fe_{0.2}O_{3-\delta}$ powder has been prepared successfully by a novel sol–gel thermolysis method. The cubic perovskite $(Ba_{0.5}Sr_{0.5})Co_{0.8}Fe_{0.2}O_{3-\delta}$ was forms at temperature as low as 450 °C, and a well-crystallized cubic perovskite form could be obtained by calcination at 650 °C for 5 h. This calcination temperature is relatively lower and the duration of calcination is relatively shorter than those of conventional solid-state reaction methods. In addition, electrical conductivity measurement revealed that the maximum conductivity of 32 S cm^{-1} was obtained in air at 500 °C, which is higher than the reported values. Obviously, $(Ba_{0.5}Sr_{0.5})Co_{0.8}Fe_{0.2}O_{3-\delta}$ can begins to loss lattice oxygen at a lower temperature of 200 °C, which is much lowered when compared with other cathode materials like LSCF [18]. Consequently, the ionic conduction is improved due to the increase of oxygen vacancies. This is the probable reason for $(Ba_{0.5}Sr_{0.5})Co_{0.8}Fe_{0.2}O_{3-\delta}$ to exhibit more remarkable electrochemical performance than LSCF even at low temperature (500–600 °C). It indicates that $(Ba_{0.5}Sr_{0.5})Co_{0.8}Fe_{0.2}O_{3-\delta}$ could be used as a good candidate for IT-SOFC cathode material.

Acknowledgement

The authors thank Professor T. Vasudevan, Head, Department of Industrial Chemistry, for encouragement and support.

References

[1] S.P. Simner, J.P. Shelton, M.D. Anderson, J.W. Stevenson, Solid State Ionics 161 (2003) 11.
[2] T.A. Damberger, J. Power Sources 71 (1998) 45.
[3] S.C. Singhal, Sold State Ionics 135 (2000) 305.
[4] R.N. Basu, F. Tietz, O. Teller, E. Wessel, J. Solid State Electrochem. 7 (2003) 416.
[5] M. Koyama, C.J. Wen, T. Masuyama, J. Otomo, H. Fukunaga, K. Yamada, K. Eguchi, H. Takahashi, J. Electrochem. Soc. 148 (2001) A795.
[6] S.P. Simner, J.E. Bonnett, N.L. Canfield, K.D. Meinhardt, J.P. Shelton, V.L. Sprenkle, J.W. Stevenson, J. Power Sources 113 (2003) 1.
[7] M.T. Colomer, B.C.H. Steele, J.A. Kilner, Solid State Ionics 147 (2002) 41.
[8] F. Zheng, L.R. Pederson, J. Electrochem. Soc. 146 (1999) 2810.
[9] R.A. De Souza, J.A. Kilner, Solid State Ionics 106 (1998) 175.
[10] Z. Shao, S.M. Haile, Nature 431 (2004) 170.
[11] L. Tan, X. Gu, L. Yang, W. Jin, L. Zhang, N. Xu, J. Membr. Sci. 212 (2003) 157.
[12] S. Lee, Y. Lim, E.A. Lee, H.J. Hwang, J.W. Moon, J. Power Sources 157 (2006) 848.
[13] B. Wei, Z. Lu, S.Y. Li, Y.Q. Liu, K.Y. Liu, W.H. Su, Electrochem. Solid State Lett. 8 (2005) A428.
[14] A. Subramania, N. Angayarkanni, T. Vasudevan, J. Power Sources 158 (2006) 1410.
[15] S.R. Jain, K.C. Adiga, V.R. Pai Verneker, Combust. Flame 40 (1981) 71.
[16] S. Ekambaram, K.C. Patil, M. Maaza, J. Alloys Compd. 393 (2005) 81.
[17] B.E. Warren, X-ray Diffraction, Dover, New York, 1990, p. 251.
[18] L.W. Tai, M.M. Nasrallash, H.U. Anderson, D.M. Sparlin, S.R. Sehlin, Solid State Ionics 76 (1995) 259.
[19] G.Vh. Kostogloudis, P. Fertis, Ch. Ftikos, J. Eur. Ceram. Soc. 18 (1998) 2009.
[20] G. Carter, A. Selcuk, R.J. Chater, J. Kajda, J.A. Kilner, B.C.H. Steele, Solid State Ionics 53 (1992) 597.